Development of a New Four Node Quadrilateral Element for a Better Bending Behavior

Dan Chandler, Volkan Isbuga, Siamak Sattar

Abstract

This study focuses on the development of a four-node quadrilateral ring element optimized to avoid locking problems exhibited by standard Iso-P elements under bending. Locking of axisymmetric elements is discussed in chapter 11 of the course material [1]. Two separate attempts will be made to address these problems. Method one involves modifying the Iso-P element by applying selective reduced integration. Method two will implement a Hellinger-Reissner (HR) formulation as opposed to the total potential energy approach (TPE). Results will be compared to those produced using standard Iso-P elements as well as analytical solutions.

Introduction

There are many limitations to the standard Iso-P element. As mentioned in AFEM chapter 22 [1], the Iso-P element is not applicable to the problems having a variational index greater than one in displacement. As a result it cannot capture the behavior of Bernoulli-Euler beams or Kirchhoff plates and shells. Although deflections computed using Iso-P elements will be of the right shape, displacement values will be significantly smaller than expected. This phenomenon is called shear locking, and results from energy being spent in shear instead of bending [1].

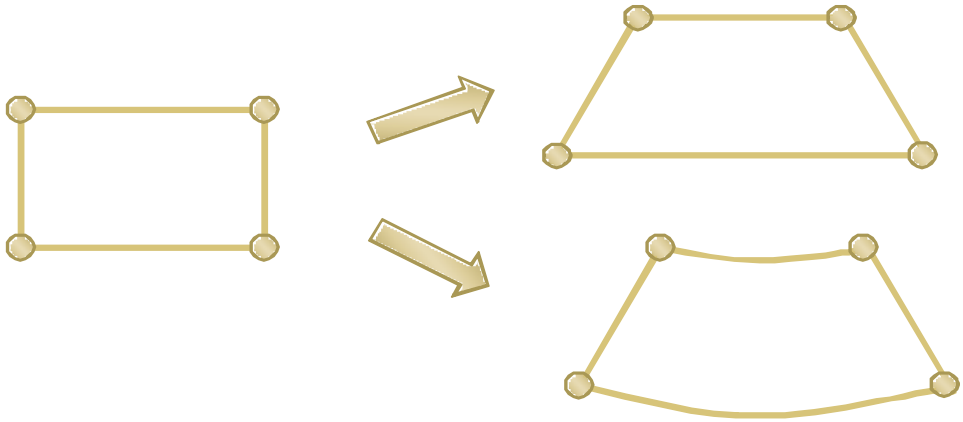

Figure 1: Shear locking vs. expected: The element on the left should undergo the deformation displayed in the lower figure. However under shear locking the shape will be similar to the upper figure.

Axisymmetric Formulation

Because this is an axisymmetric problem everything will be written in terms of cylindrical coordinates. As a result there are only four non-zero stress and strain components, which are written as 4 x 1 vectors below:

(1) Strain : $\mathbf{e} = [e_{rr} \quad e_{zz} \quad e_{\theta\theta} \quad 2e_{rz}]^T$

(2) Stress : $\boldsymbol{\sigma} = [\sigma_{rr} \quad \sigma_{zz} \quad \sigma_{\theta\theta} \quad \sigma_{rz}]^T$

(3)

$$\mathbf{E} = \frac{E_m}{(1+\nu)(1-2\nu)} \begin{bmatrix} 1-\nu & \nu & \nu & 0 \\ \nu & 1-\nu & \nu & 0 \\ \nu & \nu & 1-\nu & 0 \\ 0 & 0 & 0 & \frac{1}{2}(1-2\nu) \end{bmatrix}$$

.

Displacement functions can be approximated by shape functions multiplying nodal displacements:

(4)

$$[\mathrm{u_r(r,z)} \quad \mathrm{u_z(r,z)}]^{\mathrm{T}} = \begin{bmatrix} N_1 & 0 & N_2 & 0 & N_3 & 0 & N_4 & 0 \\ 0 & N_1 & 0 & N_2 & 0 & N_3 & 0 & N_4 \end{bmatrix} \begin{bmatrix} d_{1r} \\ d_{1z} \\ \vdots \\ d_{4z} \end{bmatrix}_{8\mathrm{x}1}$$

The matrix below is used to relate the stress and strain vectors and can be derived from the stress strain relation:

(5)

$$\mathbf{D} = \begin{bmatrix} \frac{\partial}{\partial \mathrm{r}} & 0 & \frac{1}{\mathrm{r}} & \frac{\partial}{\partial \mathrm{z}} \\ 0 & \frac{\partial}{\partial \mathrm{z}} & 0 & \frac{\partial}{\partial \mathrm{r}} \end{bmatrix}^{\mathrm{T}}$$

Hellinger- Reissner (HR) Formulation

The Hellinger Reissner approach involves a mixed formulation that approximates stresses as well as displacements. Displacements will be approximated using shape functions as is typically done when using the total potential energy functional. Stresses however will be represented in terms of constant stress parameters a_i and coordinates r and z. Element rank is equal to the number of degrees of freedom subtracted by the number of rigid body modes. For the case of a four-node quad under axial symmetry conditions the correct rank is seven. As a result the following analysis will make use of seven stress parameters.

(6) $$\boldsymbol{\sigma} = \mathbf{Sa}$$

The parameters are written in matrix form as a 7 x 1 array containing a_i. The coefficient matrix **S** is a 4 x 7 array that depends globally on r. Local dependence on r and z in **S** is written in terms of distances from the element centroid.

(7) $$\mathbf{a} = [a_1 \quad a_2 \quad a_3 \quad a_4 \quad a_5 \quad a_6 \quad a_7]^T$$

(8)

$$\mathbf{S} = \begin{bmatrix} 1 & 0 & 0 & \bar{r} & \bar{z} & 0 & 0 \\ 0 & 1 & -\dfrac{\bar{z}}{r} & 0 & 0 & \bar{r} & \dfrac{-(r+\bar{r})\bar{z}}{r} \\ 1 & 0 & 0 & r+\bar{r} & \bar{z} & 0 & 0 \\ 0 & 0 & 1 & 0 & 0 & 0 & \bar{r} \end{bmatrix}$$

(9) $$\bar{r} = r - r_0,\ r_0 = r \longrightarrow \text{centroidal coordinate of element}$$

(10) $$\bar{z} = z - z_0,\ z_0 = z \longrightarrow \text{centroidal coordinate of element}$$

These definitions can now be inserted into the Hellinger- Reissner functional which is given as:

(11) $$\Pi_{HR} = \int \left(\sigma_{ij} e_{ij} - \frac{1}{2}\sigma_{ij} C_{ijkl} \sigma_{kl} - b_i u_i\right) dV - \int \bar{t}_i u_i dS$$

Writing stresses in terms of **Sa** and displacements in terms of shape functions and nodal values gives

(12)

$$\Pi_{HR} = \mathbf{a}^{\mathrm{T}}\left(\int \mathbf{S}^{\mathrm{T}}\mathbf{D}\mathbf{N}\, dV\right)\mathbf{d} - \mathbf{a}^{\mathrm{T}}\left(\int \mathbf{S}^{\mathrm{T}}\mathbf{C}\mathbf{S}\, dV\right)\mathbf{a} - \left(\int \bar{\mathbf{t}}^{\mathrm{T}}\mathbf{N}\, dS\right)\mathbf{d}$$

Defining some compact notation:

(13)

$$\mathbf{G} = \int \mathbf{S}^{\mathrm{T}}\mathbf{D}\mathbf{N}\, dV \qquad \mathbf{F} = \int \mathbf{S}^{\mathrm{T}}\mathbf{C}\mathbf{S}\, dV \qquad \mathbf{f} = \int \bar{\mathbf{t}}^{\mathrm{T}}\mathbf{N}\, dS$$

The HR functional can now be rewritten in compact form:

(14)
$$\Pi_{HR} = \mathbf{a}^{\mathrm{T}}\mathbf{G}\mathbf{d} - \mathbf{a}^{\mathrm{T}}\boldsymbol{F}\mathbf{a} - \mathbf{f}\mathbf{d}$$

This result contains both unknown stress parameters and displacements. In order to reduce the size of the problem we can eliminate the stress parameters by minimizing with respect to **a**:

(15)
$$\frac{\partial \Pi_{HR}}{\partial \mathbf{a}} = \mathbf{G}\mathbf{d} - \mathbf{F}\mathbf{a} = \mathbf{0} \Longrightarrow \mathbf{a} = \mathbf{F}^{-1}\mathbf{G}\mathbf{d}$$

Minimizing Π_{HR} again with respect to **d** gives the final set of linear equations in the form of a traditional finite element problem:

(16)
$$\frac{\partial \Pi_{HR}}{\partial \mathbf{d}} = \mathbf{G}^{\mathrm{T}}\mathbf{a} - \mathbf{f} = \mathbf{0} \Longrightarrow \mathbf{f} = \mathbf{G}^{\mathrm{T}}\mathbf{F}^{-1}\mathbf{G}\mathbf{d}$$

(17)
$$\mathbf{f} = \boldsymbol{K}\boldsymbol{d}$$

The stiffness matrix **K** takes on the following definition:

(18) $$\boldsymbol{K} = \mathbf{G}^{\mathbf{T}}\mathbf{F}^{-\mathbf{1}}\mathbf{G}$$

Selective Reduced Formulation (SRI)

The selective reduced integration approach is straightforward in application. Derivation of the finite element equations is nearly identical to the standard Iso-P element and begins similarly with the total potential energy formulation:

(19) $$\Pi_{TPE} = \int \left(\sigma_{ij} e_{ij} - b_i u_i\right) dV - \int \bar{t}_i u_i dS$$

This equation given above can be rewritten in matrix form in the absence of body forces as:

(20)

$$\Pi_{TPE} = \mathbf{d}^{\mathrm{T}} \left(\int \mathbf{B}^{\mathrm{T}} \mathbf{E} \mathbf{B} \, dV \right) \mathbf{d} - \left(\int \bar{\mathbf{t}}^{\mathrm{T}} \mathbf{N} \, dS \right) \mathbf{d}$$

where **B** is defined in (21) below:

(21) $$\mathbf{B} = \mathbf{D}\mathbf{N}$$

Minimizing with respect to **d** produces the final set of equations used in finite element code:

(22) $$\frac{\partial \Pi_{TPE}}{\partial \mathbf{d}} = 0 \Rightarrow \mathbf{f} = \mathbf{K}\mathbf{d}$$

where (22) makes use of the definitions below:

(23) $$\mathbf{K} = \int \mathbf{B}^{\mathrm{T}} \mathbf{E} \mathbf{B} \, dV$$

$$\mathbf{f} = \int \bar{\mathbf{t}}^{\mathrm{T}} \mathbf{N}\, dS \tag{24}$$

For application of reduced integration the material matrix must first be decomposed into its deviatoric and volumetric parts. This decomposition allows the stiffness matrix to be divided into two integrals, at which point one may decide to use less Gauss points selectively in one or the other. To tackle the problem of shear locking a one-point Gauss rule is applied to the deviatoric part while the full two-point rule is retained for the volumetric stiffness matrix integral. For volumetric locking problems where $\upsilon \sim 0.5$ (incompressible materials), reduced integration is instead applied to the volumetric part of **K** [2]. In the case of shear locking a one-point rule is applied to deviatoric part because it is capable of capturing the spurious shear mode.

Decomposition of the material matrix is done in the following manner:

(25)

$$\mathbf{E} = \mathbf{E_V} + \mathbf{E_D}$$

(26)

$$\mathbf{E_V} = \frac{E_m \nu}{(1+\nu)(1-2\nu)} \begin{bmatrix} 1 & 1 & 1 & 0 \\ 1 & 1 & 1 & 0 \\ 1 & 1 & 1 & 0 \\ 0 & 0 & 0 & 0 \end{bmatrix}$$

(27)

$$\mathbf{E_D} = \frac{E_m}{2(1+\nu)} \begin{bmatrix} 2 & 0 & 0 & 0 \\ 0 & 2 & 0 & 0 \\ 0 & 0 & 2 & 0 \\ 0 & 0 & 0 & 1 \end{bmatrix}$$

The stiffness matrix is now divided into two separate integrals:

(28)

$$\mathbf{K} = \mathbf{K_V} + \mathbf{K_D} = \int \mathbf{B}^T \mathbf{E_V} \mathbf{B} dV + \int \mathbf{B}^T \mathbf{E_D} \mathbf{B} dV$$

In the next section we will consider some benchmark problems to compare results obtained using HR and SRI elements vs. the standard Iso-P Quad4.

Benchmark Problems

We considered some benchmark plate problems to compare plate deflections for different boundary conditions and loading types for different elements. The analytical deflection solutions of the benchmark problems are already known for thin plates and were used as references [3][4]. The FEM models are representations of axisymmetric physical problems with the appropriate boundary conditions and load distributions applied in the form of nodal quantities. Basic assumptions, load distributions, and boundary conditions are described for each problem below.

Boundary Condition Assumptions: Displacement boundary conditions are straightforward in the case of both simply supported and clamped plates. Center nodes must be constrained in the r direction to preserve axial symmetry while at the same time be left free to move in the z direction. For the simply supported plate the midplane node on the outer boundary is constrained in the z direction to prevent the rigid body mode from being activated. The clamped plate is constrained in both r and z at all of the outer nodes.

Load Distribution on the Nodes: The axisymmetric approach is an effort to reduce the size of the problem. The result is a two dimensional element that considers quantities for a one radian slice of the entire body. Element forces are therefore computed using a factor of $1/2\pi$. This will be elaborated upon in the examples below.

Example Benchmark Problems

Five different benchmark problems were considered to test the elements derived above. Configurations are listed below:

- Case 1: Simply Supported Plate with Edge Moment
- Case 2: Simply Supported Plate with Point Load at Center
- Case 3: Simply Supported Plate with Distributed Load
- Case 4: Clamped Plate with Point Load
- Case 5: Clamped Plate with Distributed Load

Case 1: Simply Supported Plate with Edge Moment

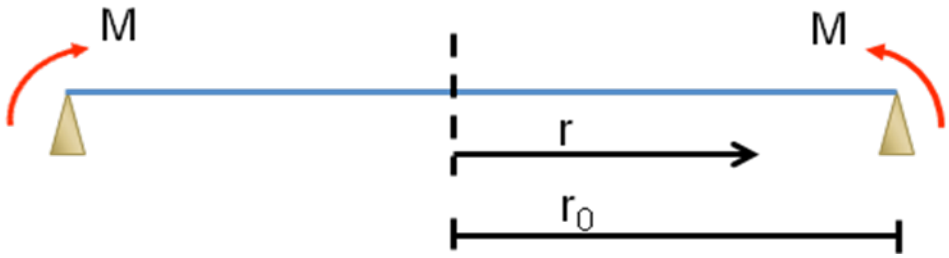

Figure 2: Problem geometry and loading

$$w(r) = \frac{M r_0^2}{2D(1+\upsilon)}\left(1-\left(\frac{r}{r_0}\right)^2\right) \quad \text{where} \quad D = \frac{E_m h^3}{12(1-\upsilon^2)}$$

$\upsilon \rightarrow$ Poisson's ratio

$h \rightarrow$ Thickness of the plate

$r_0 \rightarrow$ Radius

$M \rightarrow$ Continuous End Moment

Figure 3: Analytical solution for a simply supported plate with edge moment

Figure 4: Displacement boundary conditions.

Force Distribution on the Nodes:

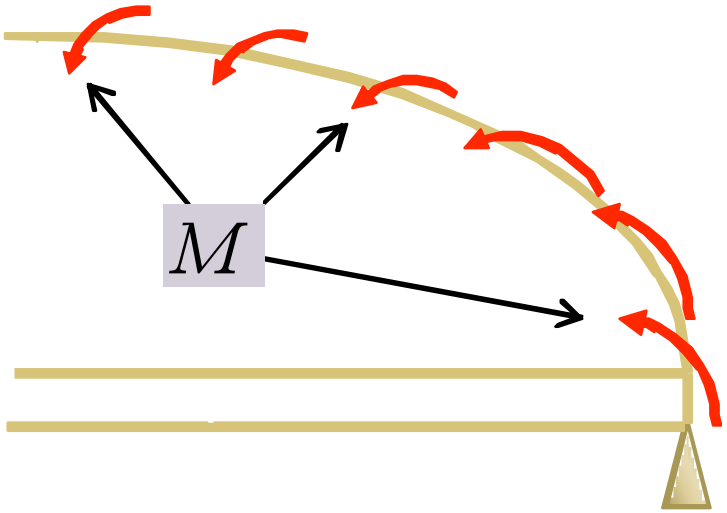

$$Fh = \frac{M(2\pi r_0)}{2\pi} = Mr_0$$

$$F = \frac{Mr_0}{h} \rightarrow \text{ Force to be used in FEM for unit radian}$$

A moment cannot be directly applied in the above finite element approach. It must be broken down into a force couple(s) that can be applied at the appropriate nodes. This is computed by first calculating the total moment acting on the circumference of the plate and dividing by 2π. This gives the total moment acting on a one-radian slice. This can be equated to an equivalent system of force couples applied at nodes. In the case of two elements in the z direction one may use the equations given above.

Results:

Em	υ	r_0	h	Load	Mesh
70 GPa	0.35	5 m	1 m	F = 100 kN	2 × 2 8 × 2

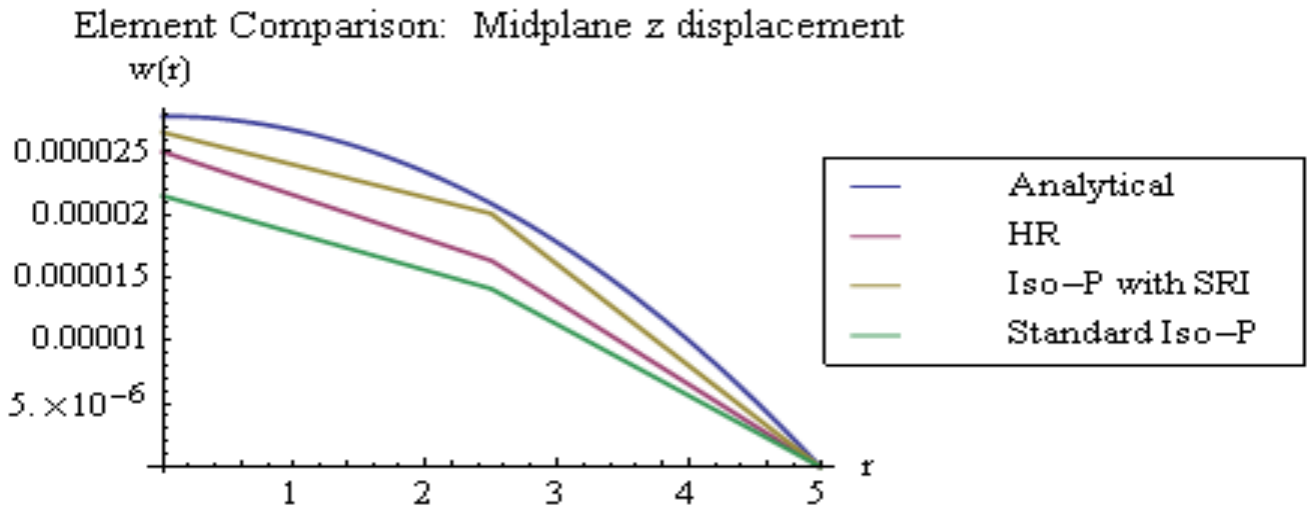

Figure 5: Simply supported plate with edge moment, 2x2 mesh, r/h = 5/1. SRI matches best, followed by HR and Iso-P. This pattern will be observed through out the benchmark analysis

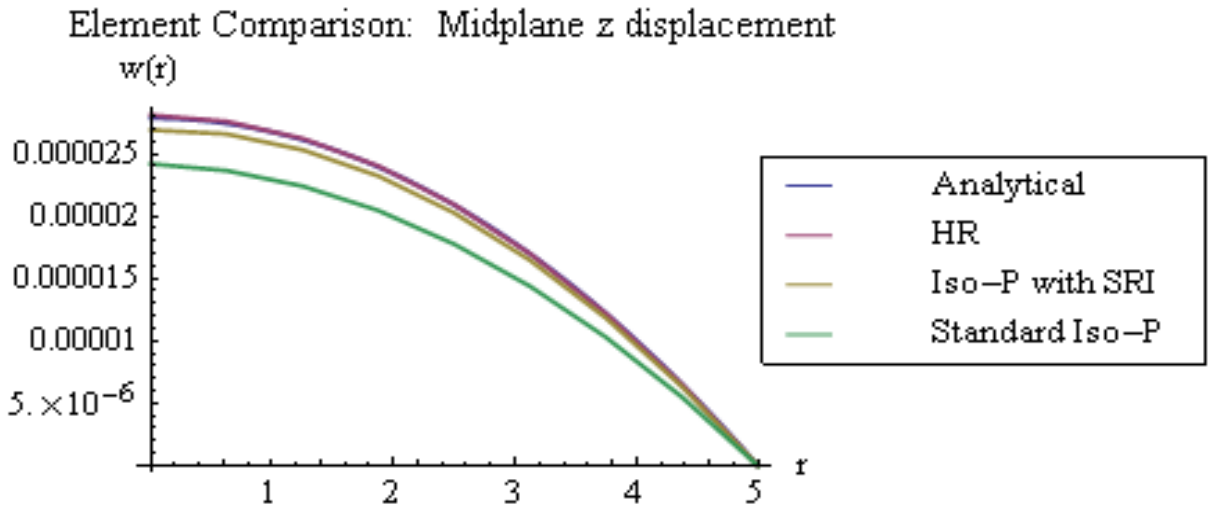

Figure 6: Simply supported plate with edge moment, 8x2 mesh, r/h = 5/1.

Em	υ	r_0	h	Load	Mesh
70 GPa	0.35	25 m	1 m	F = 100 kN	2 × 2 8 × 2

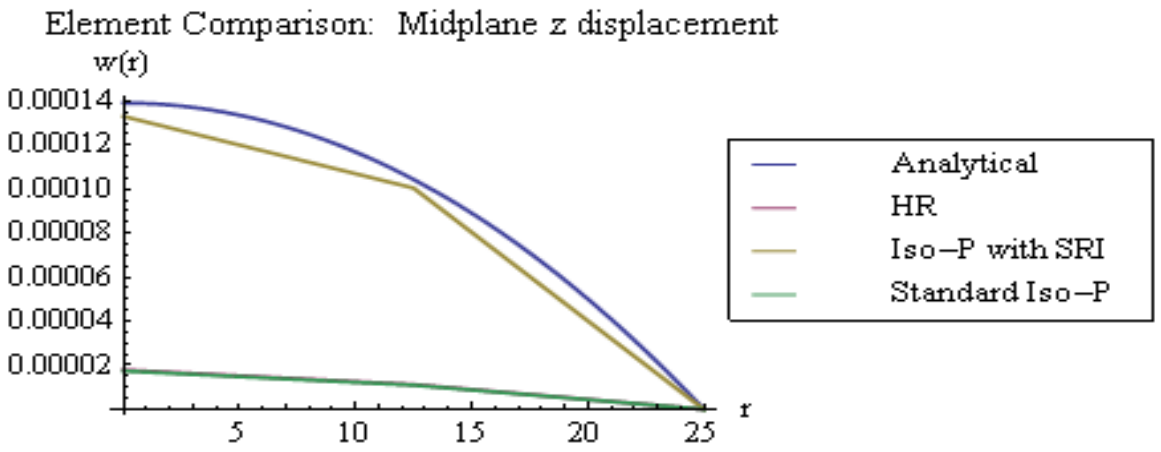

Figure 7: Simply supported plate with edge moment, 2x2 mesh, r/h = 25/1.

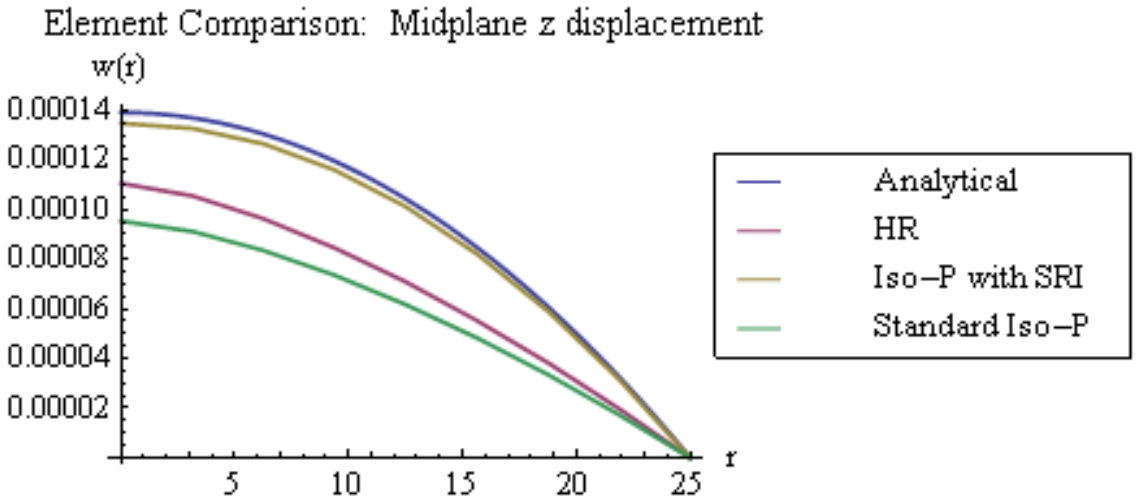

Figure 8: Simply supported plate with edge moment, 8x2 mesh, r/h = 25/1.

Case 2: Simply Supported Plate with Point Load at Center

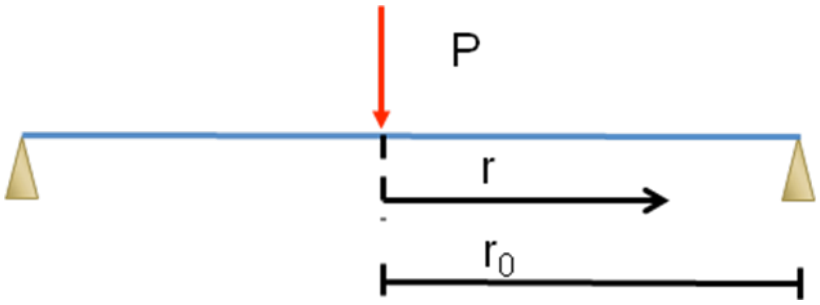

$$w(r) = \frac{Pr_0^{\,2}}{16\pi D}\left[\frac{3+\upsilon}{1+\upsilon}\left(1-\left(\frac{r}{r_0}\right)^2\right)+2\left(\frac{r}{r_0}\right)^2\ln\left(\frac{r}{r_0}\right)\right]$$

$P \rightarrow$ Point Load

Figure 9: Problem geometry and analytical solution

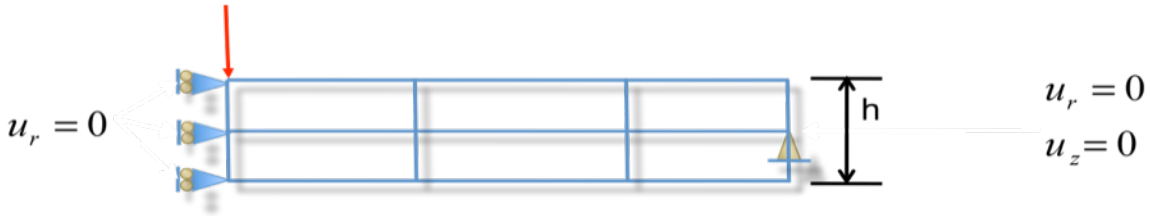

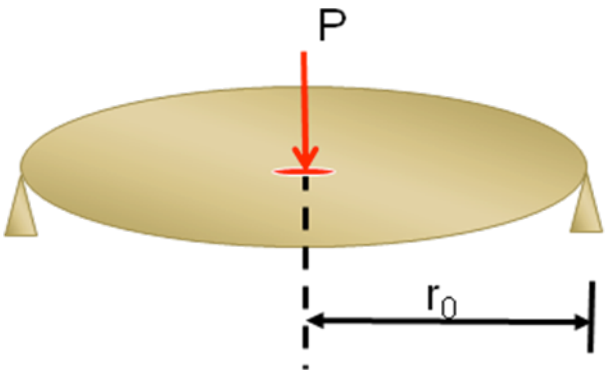

$P \rightarrow$ Acting on a small area

$F = \frac{P}{2\pi} \rightarrow$ Force to be used in FEM for unit radian

Figure 10: Displacement boundary conditions and force distribution.

Results:

Em	υ	r_0	h	Load	Mesh
70 GPa	0.35	5 m	1 m	P = 100 kN	2 × 2 8 × 2

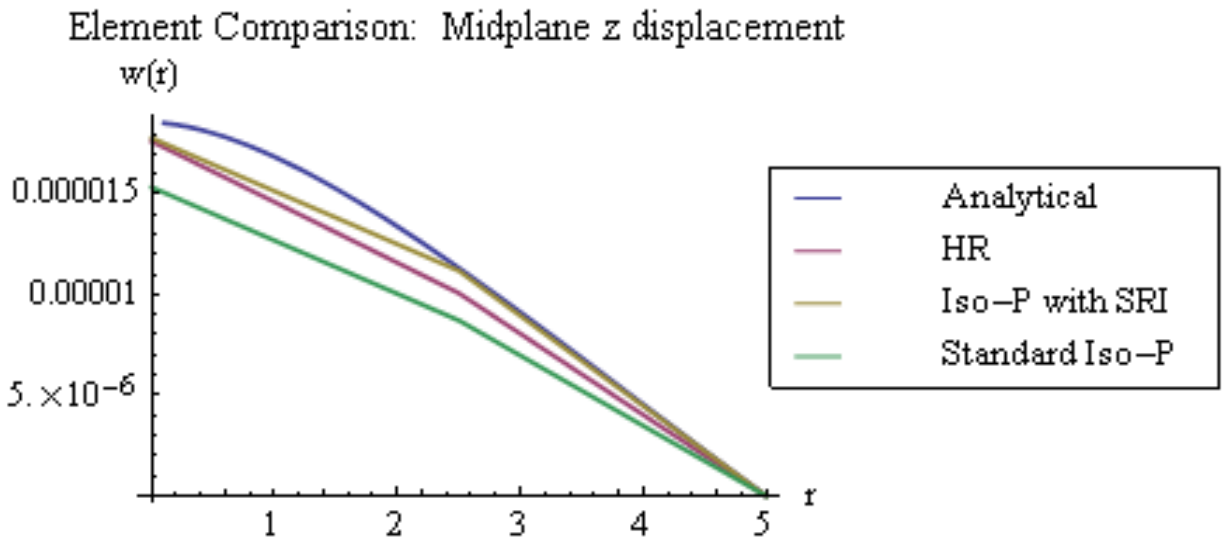

Figure 2: Simply supported plate with point load, 2x2 mesh, r/h = 5/1.

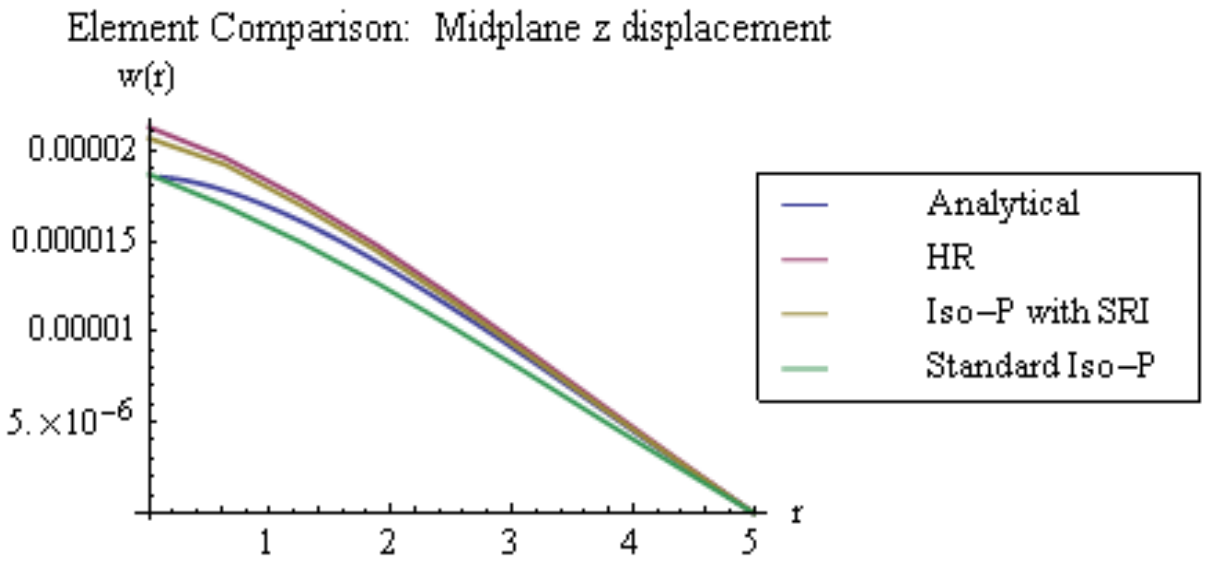

Figure 3: Simply supported plate with point load, 8x2 mesh, r/h = 5/1.

Em	υ	r_0	h	Load	Mesh
70 GPa	0.35	25 m	1 m	P = 100 kN	2 x 2 8 x 2

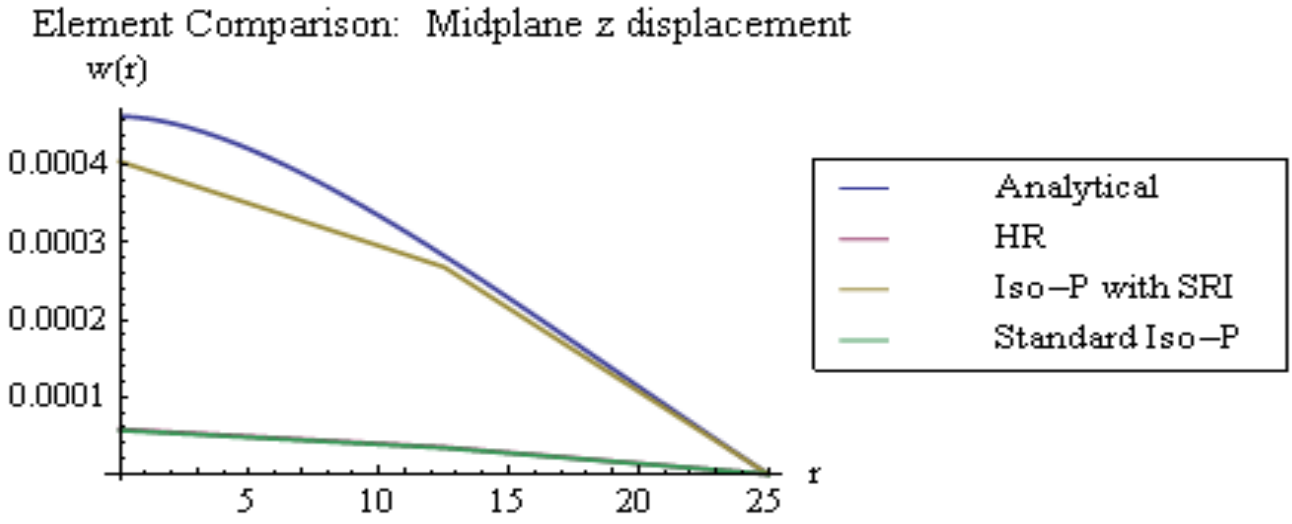

Figure 13: Simply supported plate with point load, 2x2 mesh, r/h = 25/1.

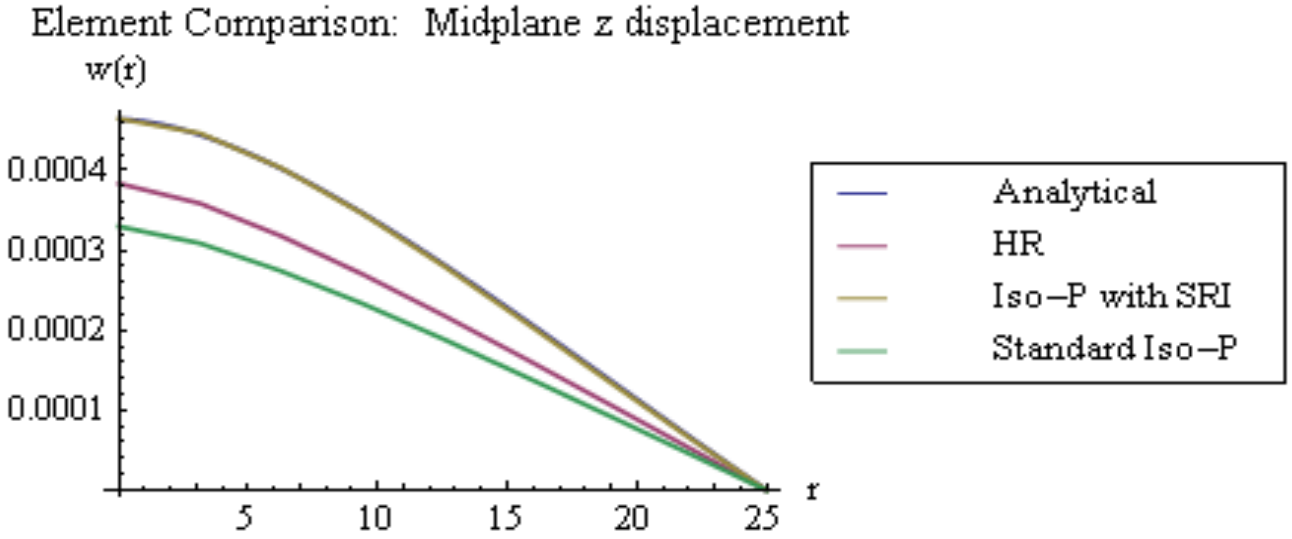

Figure 14: Simply supported plate with point load, 8x2 mesh, r/h = 25/1.

Case 3: Simply Supported Plate with Distributed Load

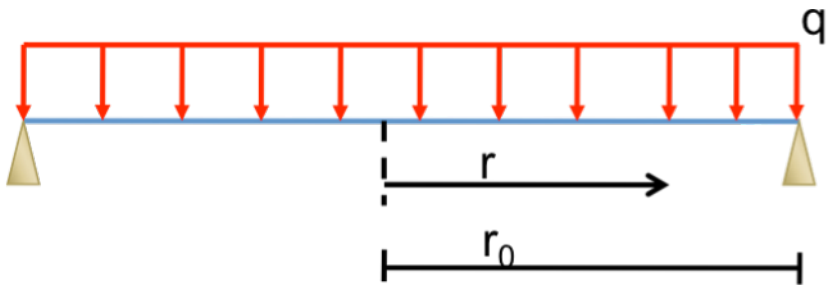

$$w(r) = \frac{q r_0^{\,4}}{64D(1+\upsilon)}\left[2(3+\upsilon)\left(1-\left(\frac{r}{r_0}\right)^2\right)-(1+\upsilon)\left(1-\left(\frac{r}{r_0}\right)^4\right)\right]$$

$$q \rightarrow \text{Distributed Load}$$

Figure 15: Problem geometry and analytical solution

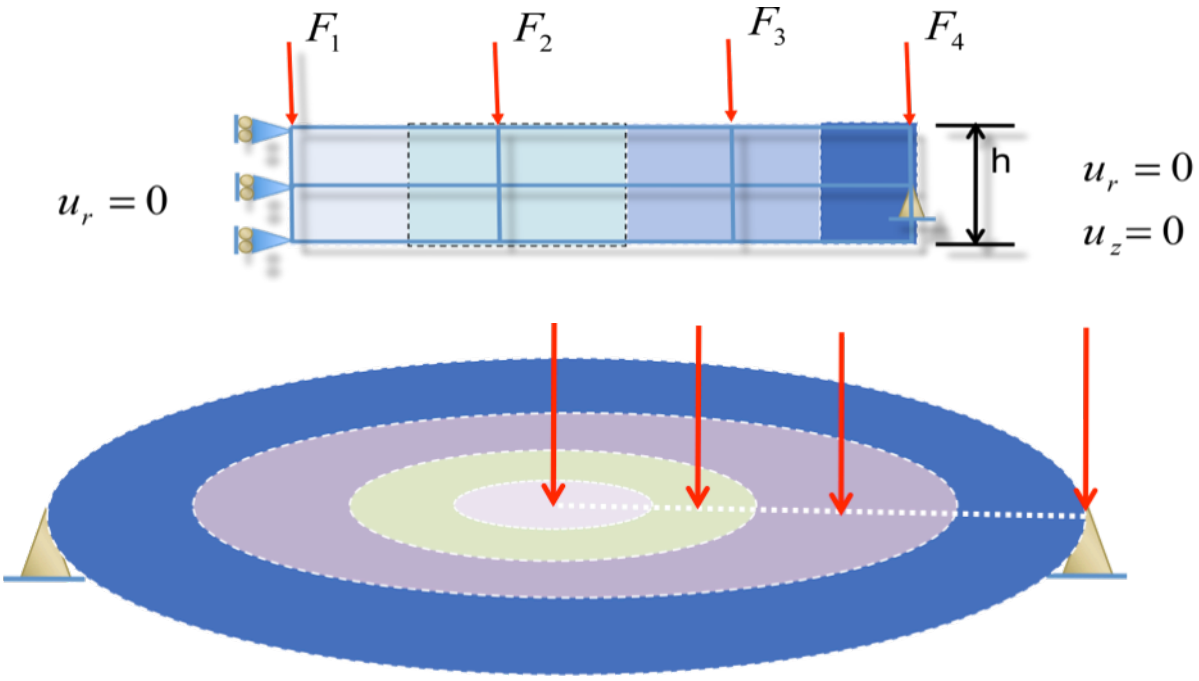

Figure 164: Displacement boundary conditions and nodal force distribution: An area of the surface is allocated to each node. Area borders were designated every half element width. The resultant force acting on a one-radian slice of area was then lumped to its respective node.

Em	υ	r_0	h	Load	Mesh
70 GPa	0.35	5 m	1 m	F = 100 kN	2 × 2 8 × 2

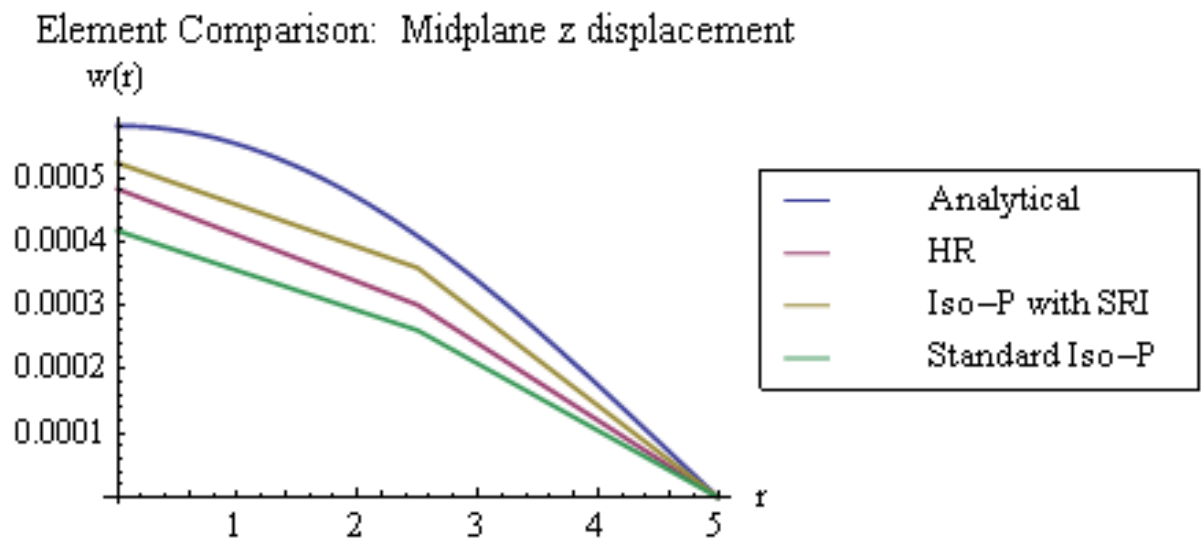

Figure 5: Simply supported plate with distributed load, 2x2 mesh, r/h = 5/1.

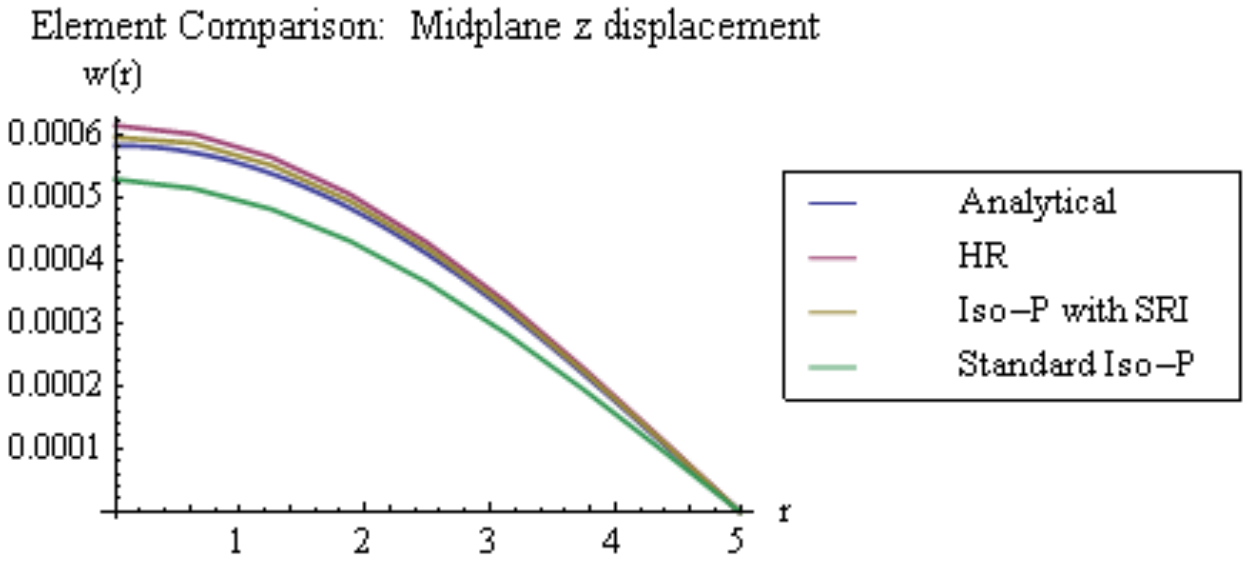

Figure 18: Simply supported plate with distributed load, 8x2 mesh, r/h = 5/1.

Em	υ	r_0	h	Load	Mesh
70 GPa	0.35	25 m	1 m	P = 100 kN	2 x 2 8 x 2

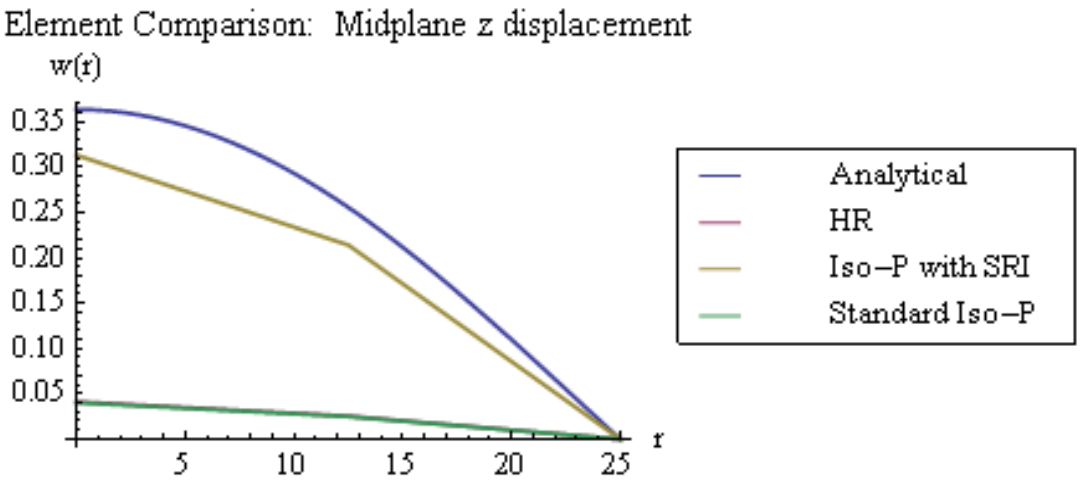

Figure 6: Simply supported plate with distributed load, 2x2 mesh, r/h = 25/1.

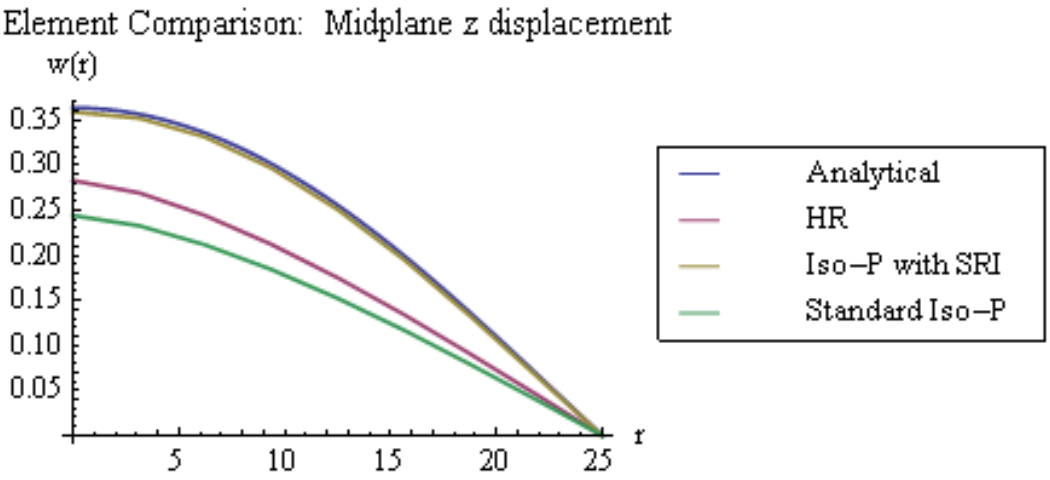

Figure 7: Simply supported plate with distributed load, 8x2 mesh, r/h = 25/1.

Case 4: Clamped Plate with Point Load

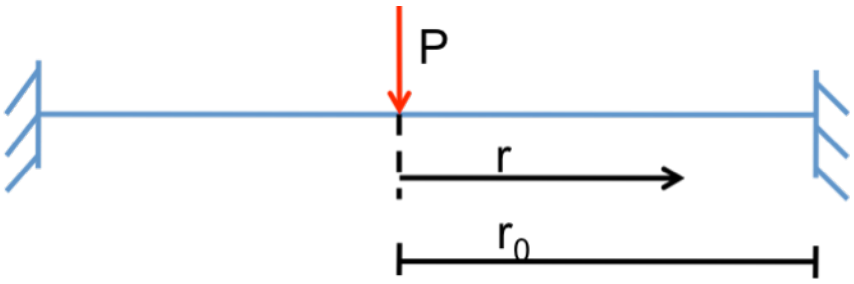

$$w(r) = \frac{\mathrm{Pr}_0^{\,2}}{16\pi D}\left[1-\left(\frac{r}{r_0}\right)^2+2\left(\frac{r}{r_0}\right)^2\ln\left(\frac{r}{r_0}\right)\right]$$

$$P \rightarrow \text{Point Load}$$

Figure 8: Problem geometry and analytical solution

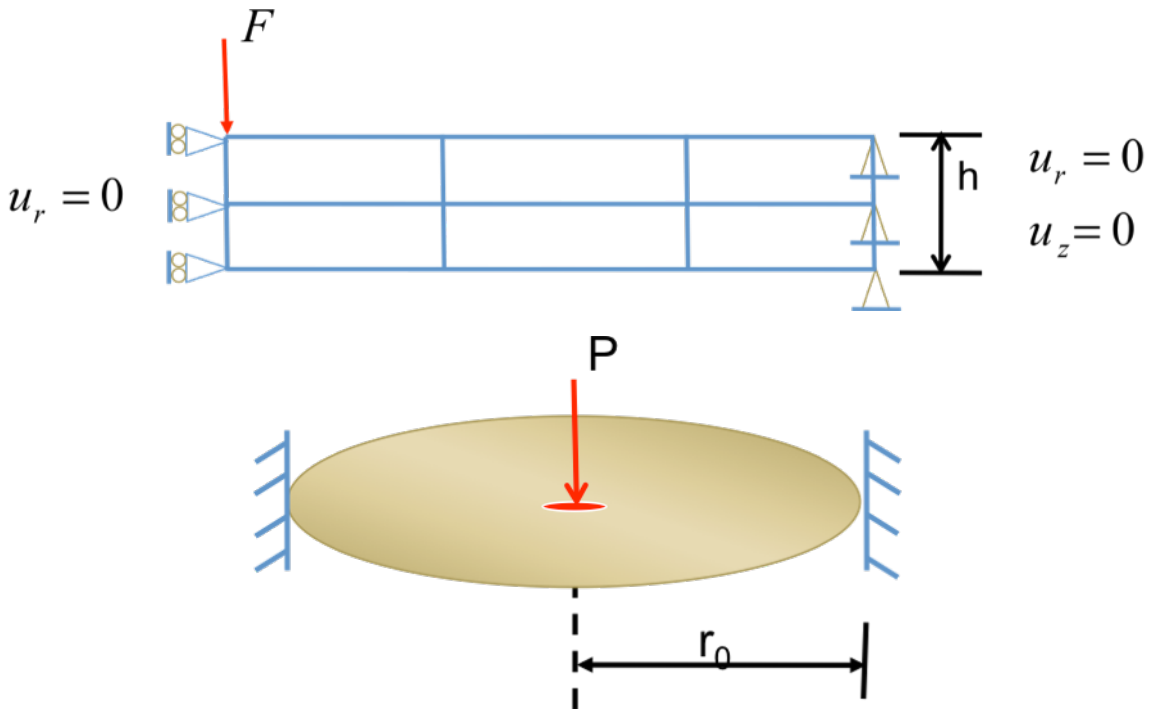

Figure 22: Displacement boundary conditions and force distribution

Em	υ	r_0	h	Load	Mesh
70 GPa	0.35	5 m	1 m	F = 100 kN	2 × 2 8 × 2

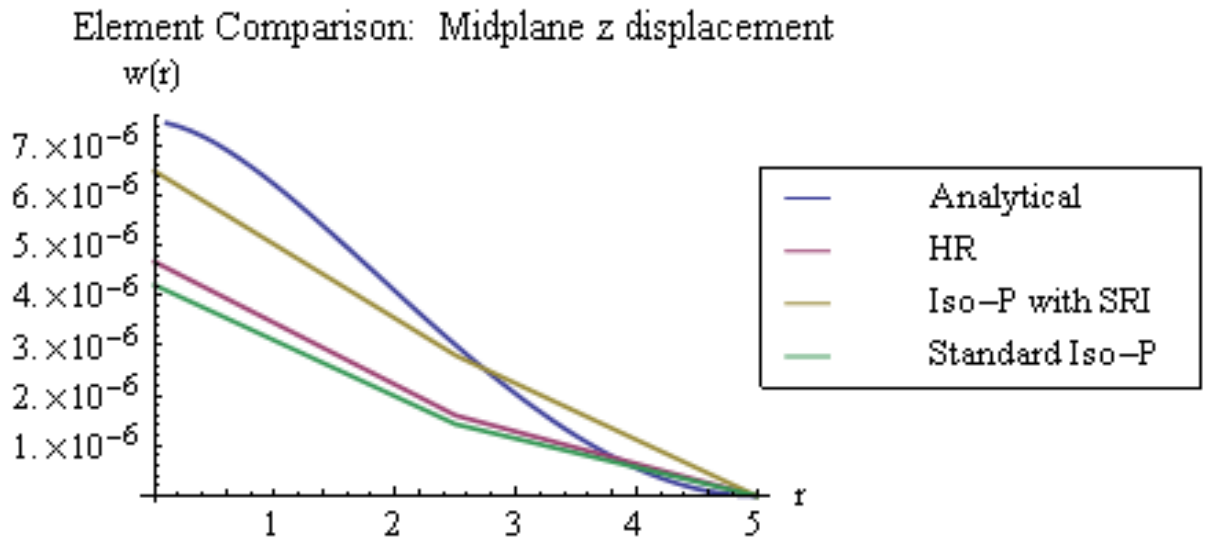

Figure 23: Clamped plate with point load, 2x2 mesh, r/h = 5/1. This is not quite an adequate mesh to describe the problem however for the sake of consistency the same meshes were used as in the previous cases. This configuration still demonstrates the order of convergence as more elements are added.

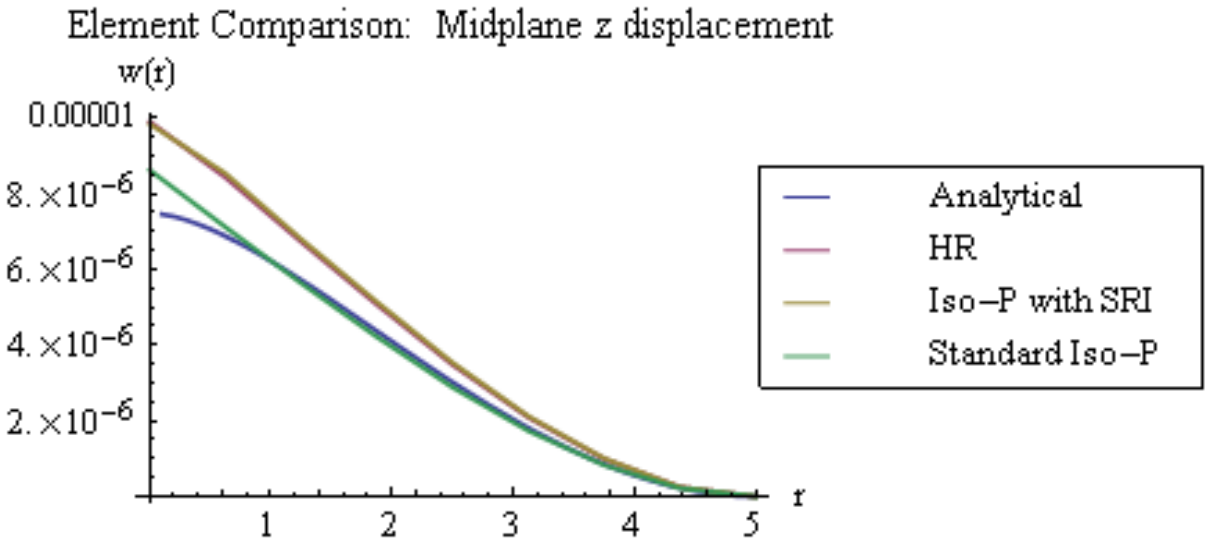

Figure 24: Clamped plate with point load, 8x2 mesh, r/h = 5/1. For the clamped plate a larger 2r/h ratio is needed for validity of the analytical solution. All results converge that of SRI as more elements are added.

Em	υ	r_0	h	Load	Mesh
70 GPa	0.35	25 m	1 m	P = 100 kN	2 x 2 8 x 2

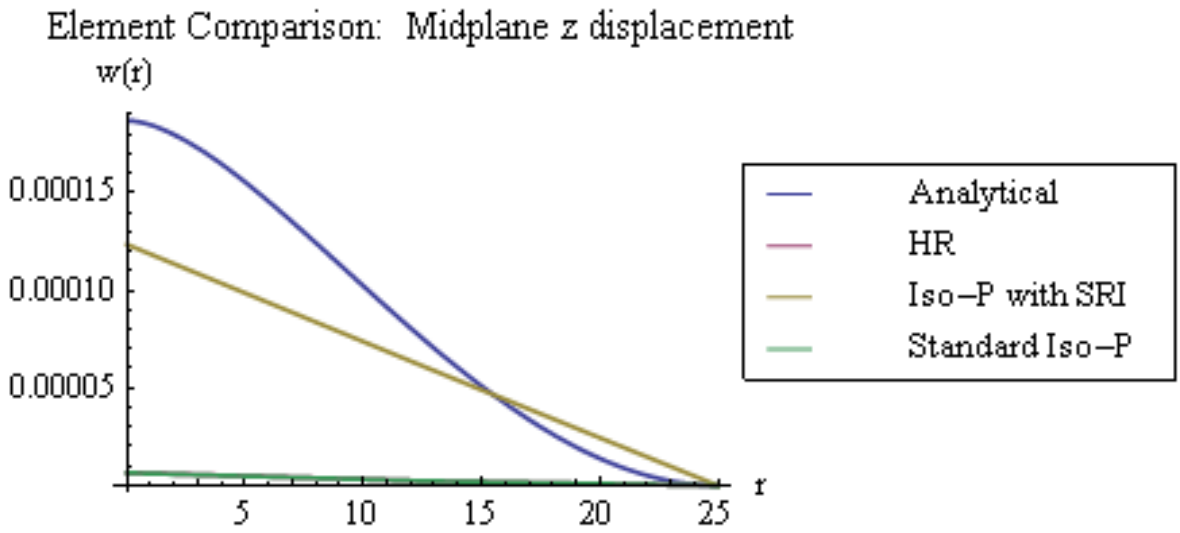

Figure 25: Clamped plate with point load, 2x2 mesh, r/h = 25/1. Again, more elements are needed here but superiority of the SRI element is adequately demonstrated.

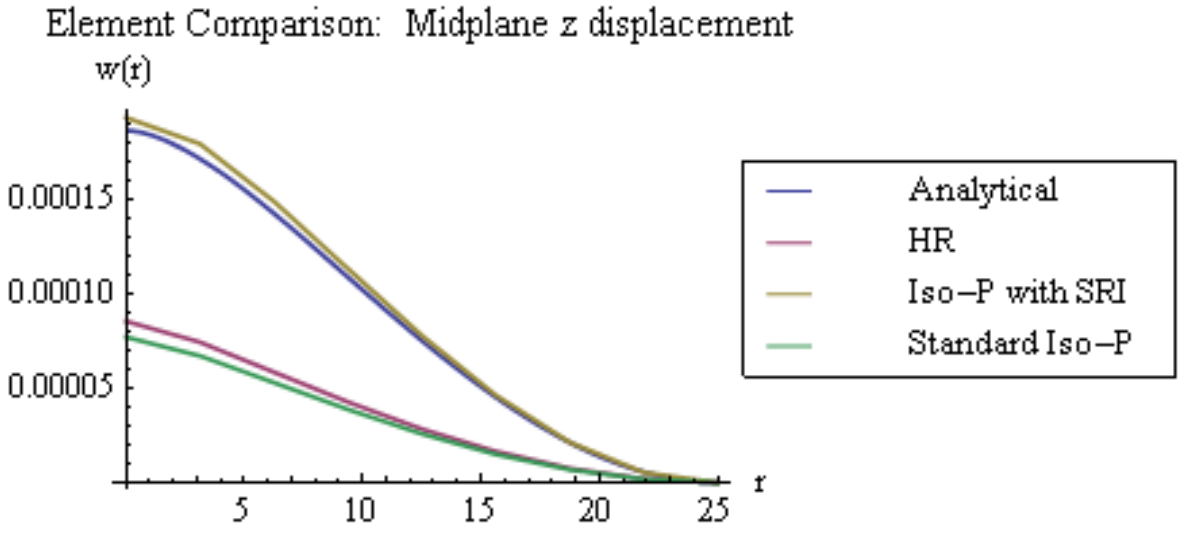

Figure 26: Clamped plate with point load, 8x2 mesh, r/h = 25/1.

Case 5: Clamped Plate with Distributed Load:

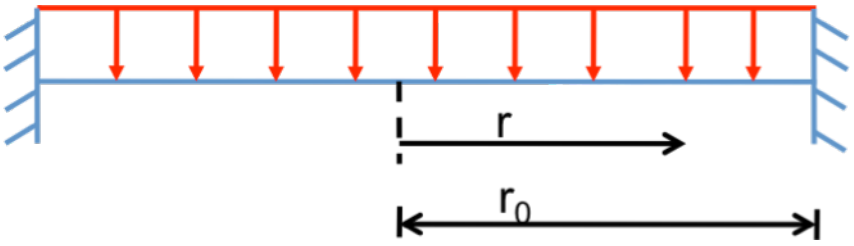

$$w(r) = \frac{q r_0^{\,4}}{64D}\left[\left(1-\left(\frac{r}{r_0}\right)^2\right)^2\right]$$

$$q \rightarrow \text{Distributed Load}$$

Figure 27: Problem geometry and analytical solution

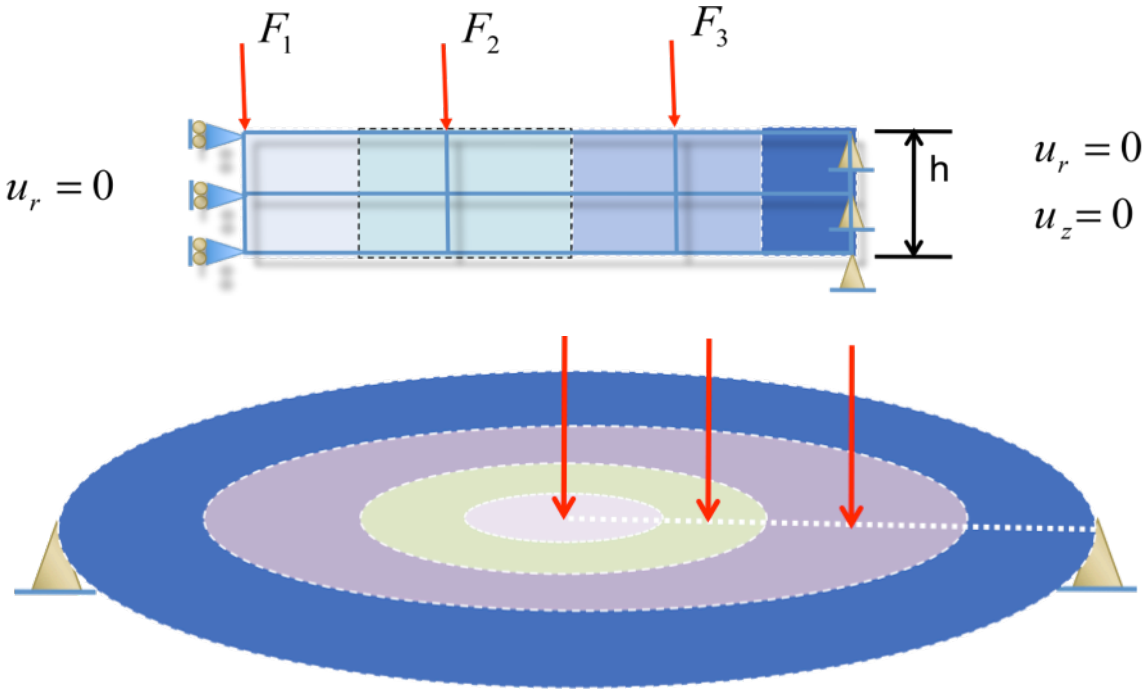

Figure 28: Force distribution is similar to that of simply supported plate with distributed load. Note that in this case the outer node has no force applied because of the clamped boundary condition on the upper surface node.

Em	υ	r_0	h	Load	Mesh
70 GPa	0.35	5 m	1 m	F = 100 kN	2 × 2 8 × 2

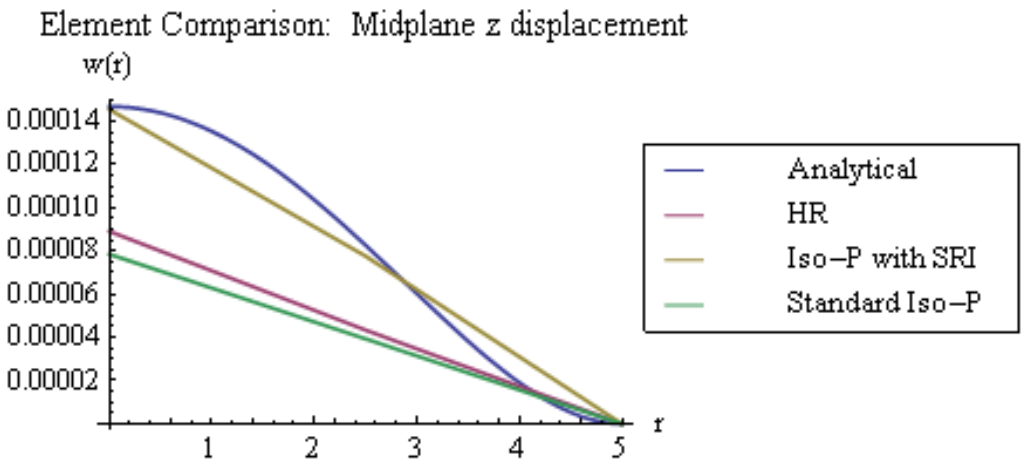

Figure 299: Clamped plate with distributed load, 2x2 mesh, r/h = 5/1.

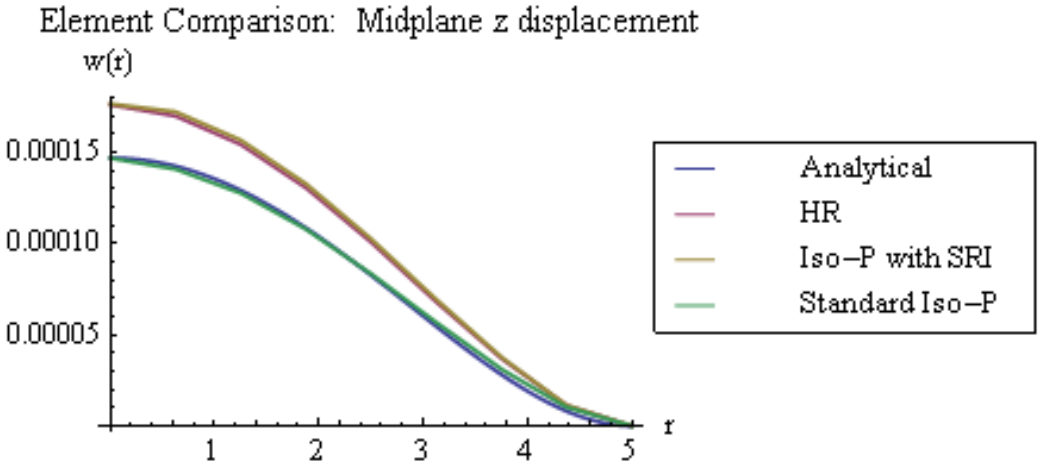

Figure 30: Clamped plate with distributed load, 8x2 mesh, r/h = 5/1.

Em	υ	r_0	h	Load	Mesh
70 GPa	0.35	25 m	1 m	P = 100 kN	2 x 2 8 x 2

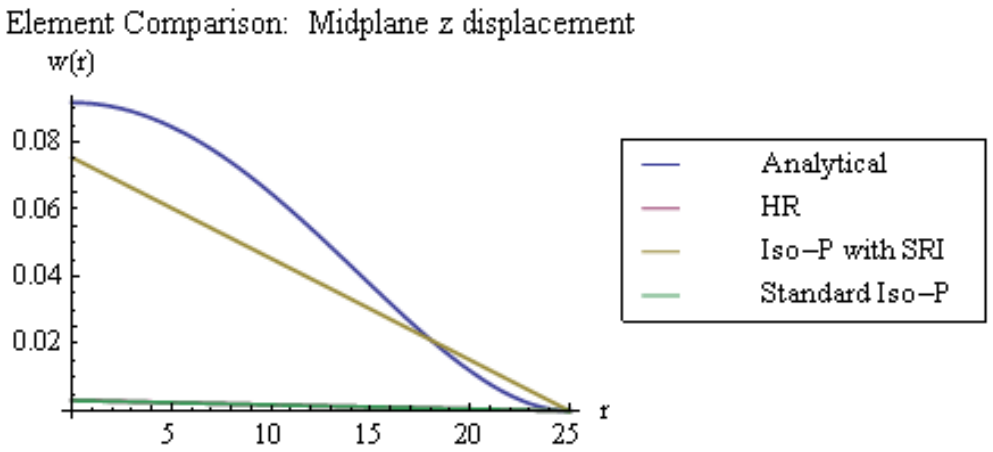

Figure 31: Clamped plate with distributed load, 2x2 mesh, r/h = 25/1.

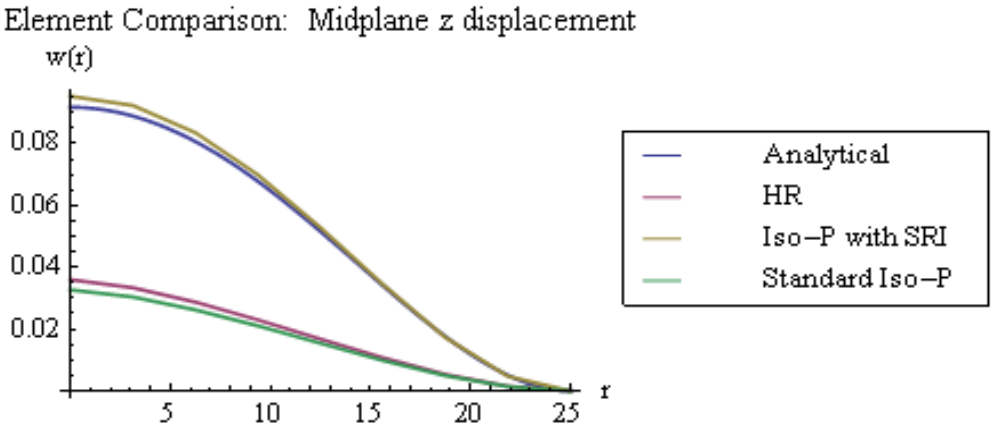

Figure 32: Clamped plate with distributed load, 8x2 mesh, r/h = 25/1.

Conclusions

It is quite evident that the SRI element is superior. Locking problems were noticeably worse in the case of thin plates but the SRI element performed as if nearly unaffected. However as Poisson's ratio approaches 0.5, results given by the SRI element will degenerate to that of a standard Iso-P while HR results converge nicely as more elements are added.

Out[2224]=

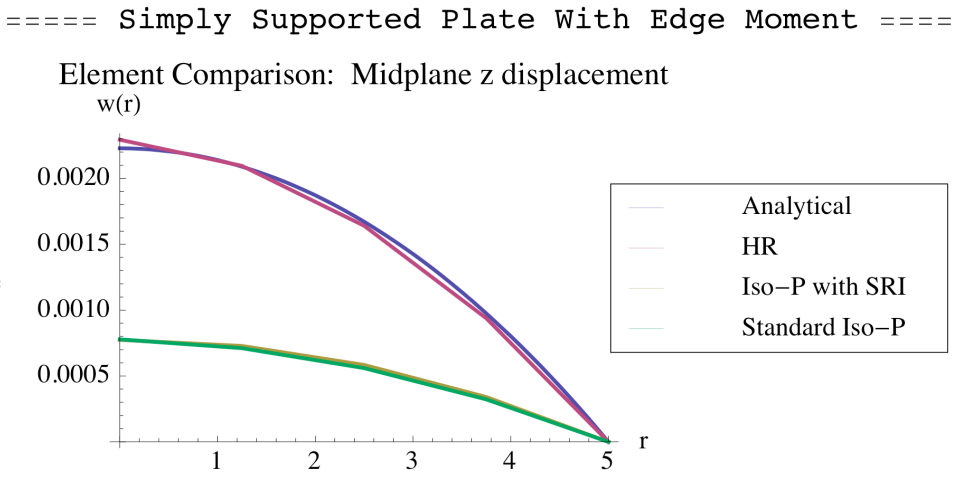

Out[2286]=

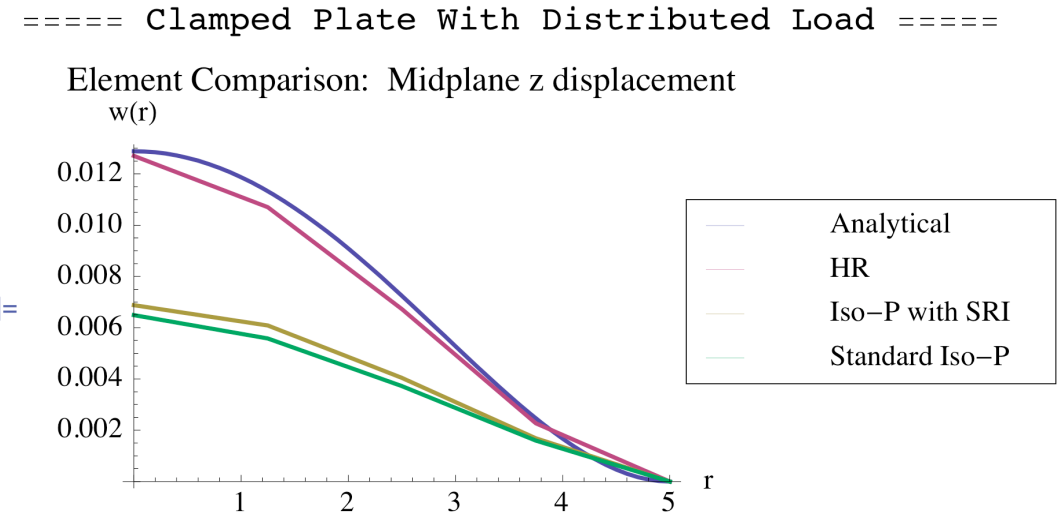

Figure 33: 4x2 mesh. This result occurs as Poisson's ratio approaches 0.5 with out changing the Gauss rule for the SRI element. HR works best, followed by SRI then Iso-P.

```
===== Simply Supported Plate With Edge Moment =====
```

Out[2842]=

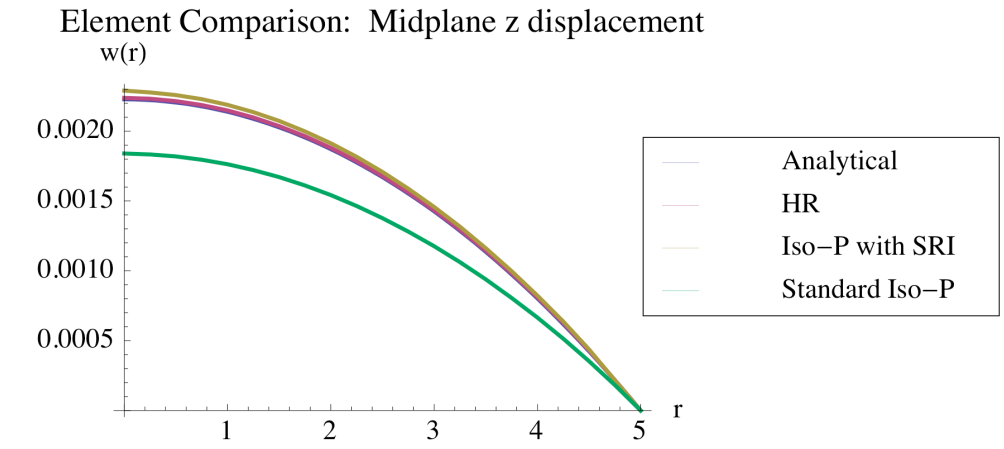

Figure 34: Switching the SRI Gauss rule and refining the mesh puts the SRI element back in the game.

If the reduced Gauss rule is removed from the deviatoric stiffness and applied to the volumetric component the SRI element once again reigns supreme.

A different combination of stress parameters may greatly improve the HR element performance. In its current guise it still significantly outperforms the standard Iso-P. Top performance using formulations in this report however goes to the SRI element. It has a simple formulation and is easy to implement in code. The SRI element's shortcomings appear with more complicated materials where **E** cannot be decomposed.

References

[1] Felippa, A. Carlos, AFEM Lecture Notes, Department of Aerospace Engineering Sciences, University of Colorado at Boulder.

[2] Hughes, T. J. R., The Finite Element Method: Linear Static and Dynamic Finite Element Analysis, Prentice Hall, Englewood Cliffs, NJ, 1987; Dover reprint, 2000.

[3] Szilard, R., Theory and Analysis of Plates, Prentice-Hall, N.J., 1974.

[4] Timoshenko, S. P. and S. Woinowsky-Krieger, S., Theory of Plates and Shells, McGraw-Hill, NewYork, 1959